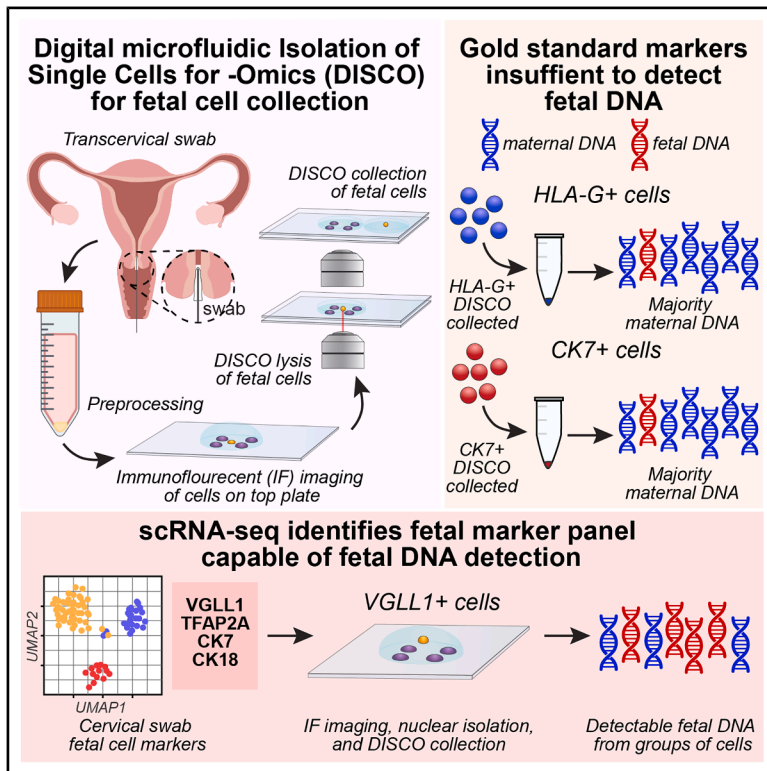


A digital microfluidic platform for cell-based non-invasive testing

Graphical abstract



Authors

Dylan Siriwardena, Michael D.M. Dryden, M. Dean Chamberlain, ..., David Chitayat, Aaron R. Wheeler, Elena Greenfeld

Correspondence

elena.greenfeld@sinaihealth.ca

In brief

Diagnostic procedure; Fluidics; Biological sciences; Developmental genetics; Omics; Biological sciences research methodologies

Highlights

- Our DISCO platform enables collection of fetal cells from transcervical swabs
- Gold standard fetal cell markers are insufficient to identify fetal cells
- scRNA-seq analysis of placenta and cervical swabs identified 147 fetal cell markers
- Nuclear isolation and DISCO collection reduces maternal DNA contamination



Article

A digital microfluidic platform for cell-based non-invasive testing

Dylan Siriwardena,^{1,2} Michael D.M. Dryden,^{1,2,3} M. Dean Chamberlain,^{1,2,4} Chloe Taylor,^{1,2} Louise Dupoirson,^{1,2} Shriya Gulati,^{1,2} Farhana Abbas,^{1,2} Julian Lamanna,^{1,2} David Chitayat,^{5,6} Aaron R. Wheeler,^{1,2,7} and Elena Greenfeld^{8,9,10,*}

¹Department of Chemistry, University of Toronto, Toronto, ON, Canada

²Donnelly Centre for Cellular and Biomolecular Research, University of Toronto, Toronto, ON, Canada

³National Research Council, Ottawa, ON, Canada

⁴Department of Oncology, University of Saskatchewan, Saskatoon, SK, Canada

⁵Department of Obstetrics & Gynaecology, Sinai Health System, Toronto, ON, Canada

⁶Department of Paediatrics, University of Toronto, Toronto, ON, Canada

⁷Institute of Biomedical Engineering, University of Toronto, Toronto, ON, Canada

⁸Division of Diagnostic Medical Genetics, Sinai Health System, Toronto, ON, Canada

⁹Department of Laboratory Medicine & Pathobiology, University of Toronto, Toronto, ON, Canada

¹⁰Lead contact

*Correspondence: elena.greenfeld@sinaihealth.ca

<https://doi.org/10.1016/j.isci.2026.116413>

SUMMARY

Gold-standard prenatal genetic diagnostics rely on invasive sampling procedures, which carry a small risk of miscarriage and do not yield results until after 14 weeks of gestation. Cervical mucosa is a promising cellular source for intact fetal cells but is limited by the paucity of fetal cells. We apply digital microfluidic isolation of single cells for omics (DISCO) to collect fetal cells from cervical mucosa for prenatal genetic diagnostics. Using gold standard markers, we collected putative fetal cells from transcervical swabs but found the material was predominantly of maternal origin. By integrating placental and transcervical swab transcriptomes, we identified a population of putative fetal cells characterized by 147 marker genes in common with fetal placental tissue. DISCO collections of prospective fetal cells contained identifiable fetal and maternal DNA. Thus, our DISCO system enabled the identification of fetal cell markers, collection of putative fetal cells, and analysis of fetal DNA.

INTRODUCTION

Non-invasive prenatal testing (NIPT) has transformed prenatal care by allowing risk assessment for select fetal genetic conditions without posing a risk to the pregnancy. Currently, prenatal diagnosis relies on invasive procedures, such as chorionic villus sampling (CVS) or amniocentesis, which, although diagnostic and highly accurate, carry a small risk of miscarriage. The introduction of NIPT using cell-free fetal DNA (cffDNA) in maternal plasma has provided a safer, highly sensitive screening method for common chromosomal aneuploidies, leading to its rapid widespread clinical adoption. Indeed, cffDNA-based NIPT has become standard for screening common aneuploidies, including trisomies 21, 18, and 13.^{1–4} Despite its advantages, cffDNA-based NIPT has critical limitations. The fetal fraction typically represents $\leq 10\%$ of total cell free DNA, resembling mosaicism and complicating detection of fetal abnormalities.^{5–8} Additionally, the fragmented nature of cffDNA further restricts comprehensive genomic interrogation.^{9–12}

Given these limitations, interest in cell-based NIPT (cbNIPT) has surged, particularly as technical advances have improved cell isolation and genetic analysis methods. cbNIPT has been

shown to be a promising diagnostic alternative with numerous studies demonstrating its potential to deliver more comprehensive genetic information.^{13–18} cbNIPT relies on two main sources of fetal cells: those isolated from maternal circulation and those retrieved from the transcervical canal. Fetal cells from both sources predominantly originate from the placenta. However, despite recent advances in microfluidic cell isolation from maternal blood,^{19–22} circulating fetal cells are extremely rare and likely to be degraded, making their recovery and analysis challenging.^{23,24} In contrast, transcervical trophoblasts are collected closer to the placental source through a procedure similar to a PAP smear and therefore thought to be more abundant and better preserved.^{13,14,16,17,25,26} Cell picking of trophoblast cell lines spiked into pap smears has been applied in principle in previous studies.²⁷ However, little is known about the molecular profiles of trophoblast cells from transcervical swabs. Moreover, common cell picking methods are slow and unable to molecularly profile target cells, while current microfluidic approaches cannot be applied to cervical mucosa samples.

In this study, we apply our digital microfluidic isolation of single cells for omics (DISCO) platform^{28,29} to isolate fetal cells from transcervical samples collected during the first trimester of



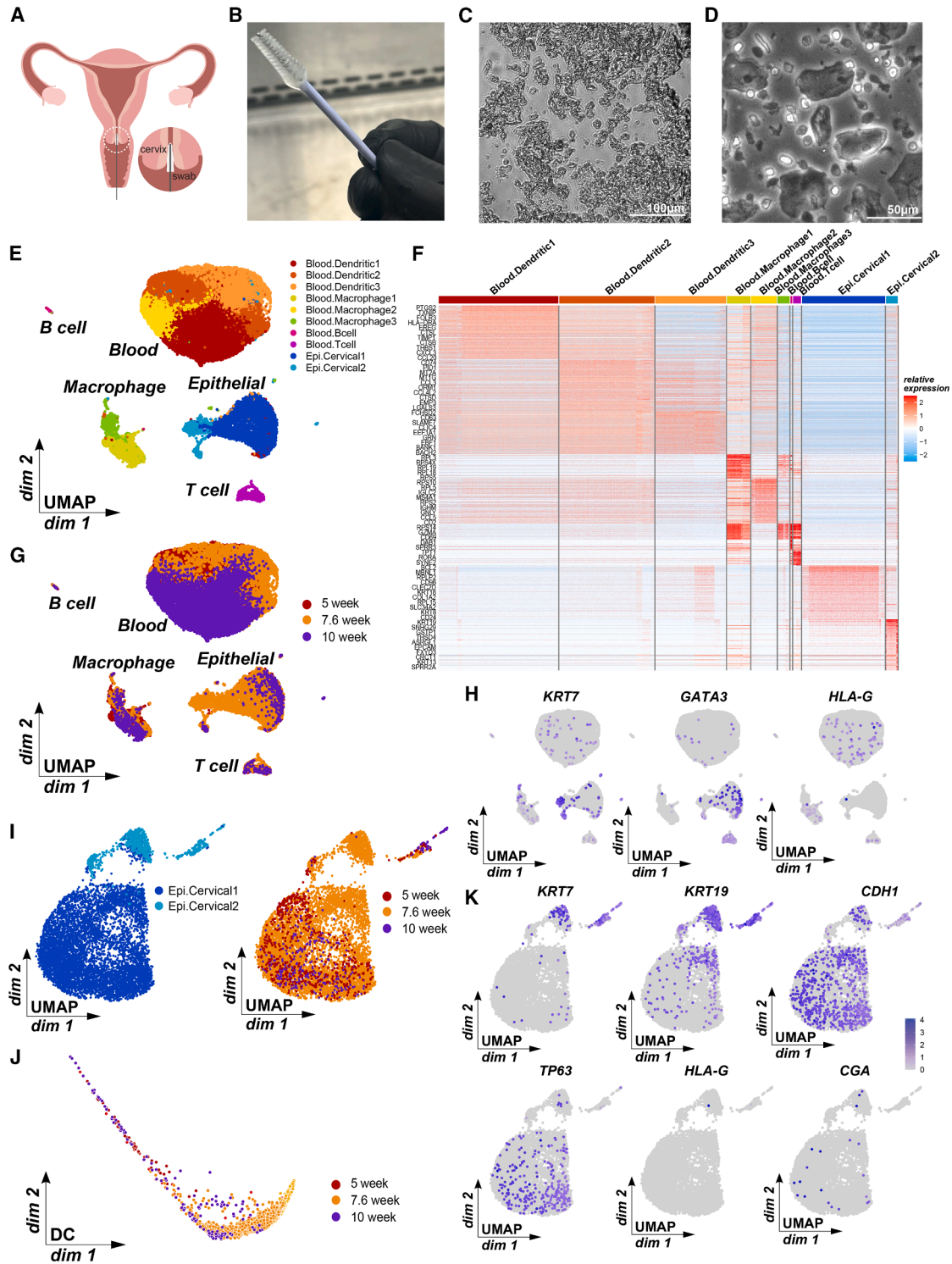


Figure 1. Single cell RNA sequencing of transcervical swabs from 5–10 weeks of gestation

- (A) Schematic of transcervical swab technique.
 (B) Photo of a transcervical swab.
 (C) Brightfield image of dissociated transcervical swab cells.
 (D) Phase contrast image of transcervical swab cells before RNA sequencing.
 (E) UMAP of merged cervical swab RNA sequencing datasets.

(legend continued on next page)

pregnancy. Collection of prospective fetal cells identified by gold standard markers CK7 or HLA-G yielded predominantly maternal DNA. RNA sequencing of transcervical swabs revealed large proportions of maternal cells expressing CK7 and HLA-G. RNA sequencing of matched placental profiles enabled the identification of 147 genes shared between fetal placenta and a subpopulation of potential fetal cells in transcervical swabs, including TFAP2A, CK7 and VGLL1. DISCO collection of VGLL1+ CK7+ and TFAP2A + CK7+, were found to contain fetal and maternal DNA. Thus, transcervical swabs represent a promising NIPT source with high potential for further improvements.

RESULTS

Single cell RNA sequencing of transcervical swabs from 5 to 10 weeks of gestation

Little is currently known of the cellular or molecular profile of transcervical swabs. To profile the cell populations captured by transcervical swabs, we performed single cell RNA sequencing of transcervical swabs from three gestational ages. Transcervical and matched placental samples were collected from women who were undergoing pregnancy termination from week 5 to week 12 (Figures 1A and 1B). DNA and RNA quality was predicated on the collection of live healthy cells in a single cell suspension. Consequently, we developed gentle mucolytic strategies to collect single cells prior to single cell RNA sequencing (Figures 1C and 1D). A variety of cellular morphologies were observable, with cellular diameters ranging from $\sim 5 \mu\text{m}$ to over $100 \mu\text{m}$ (Figure 1D).

A total of 35,234 cells were collected from bulk transcervical swabs and analyzed from three gestational ages spanning our examined cohort: week 5.2, 7.6, and 10.3. Initial clustering and uniform manifold approximation and projection (UMAP) analysis revealed ten subclusters spanning five major clusters (Figure 1E). Differential expression analysis revealed substantial blood cell and epithelial cell populations, as determined by established markers (Figure 1F). Interestingly, cervical swab cells were clustered by cell type rather than gestational age (Figure 1G).

To identify fetal cells from within our RNA sequencing dataset, we examined gold standard fetal cell markers cytokeratin 7 (gene name, KRT7; protein name, CK7) and HLA-G (Figure 1H). Notably, each of these markers identified numerous cells from differing clusters. HLA-G expression was predominantly confined to the blood cell compartment, indicating a lack of specificity for fetal cells and making it unsuitable for their isolation. (Figure 1H).

Interestingly, a subpopulation of KRT7+ cells was observable within the cervical epithelium cluster (Figure 1H). Cytotrophoblast and column cytotrophoblast are abundant in the fetal placenta during the first trimester and have epithelial character-

istics. To determine if these trophoblast subpopulations were captured in the epithelial cell cluster, we performed *de novo* clustering and multidimensional reduction analysis on epithelial cell clusters from the three gestational ages (Figure 1I). Interestingly, epithelial cell types demonstrated a lack of clustering by gestational age (Figure 1I). Diffusion map analysis further demonstrated no organization by gestation age, placing week 5.2 and 10.3 cells in closer proximity than 7.6 (Figure 1J). Therefore, we grouped epithelial cells from all three gestational ages for further subpopulation analysis. Differential expression analysis revealed the enrichment of keratins such as KRT7, KRT18, and KRT19, as well as the epithelial marker CDH1 in a subcluster of cervical epithelium, consistent with known cytotrophoblast profiles (Figure 1K).

Transcervical swabs contain HLA-G and CK7 positive cells

To characterize the cell types identified from our RNA sequencing analysis, we performed immunofluorescent staining of previously identified cell types in transcervical swabs (Figure 1E). Single cell suspensions were obtained from transcervical swabs utilizing the reducing agent DTT without fixation, maintaining cellular integrity (Figures 2A and 2B). In bulk transcervical swab suspension, epithelial and blood cells-like morphologies were identified as the predominant populations (Figure 2B). To determine if any populations were shared with placental populations, matched placental samples from the same patient were examined. Placental epithelial trophoblast shared known epithelial markers such as pan-keratin (panCK+) (Figure S1A). Epithelial cells expressed pan-keratin and varied greatly in size between $5 \mu\text{m}$ and $100 \mu\text{m}$ in diameter. CD163+ monocytes/macrophages were present in cervical swabs but absent in placental sections (Figure S1A).

Cytokeratin 7 (CK7) and HLA-G have been proposed in previous studies as reliable markers for trophoblast identification and have been employed to detect fetal cells in cbNIPT. ^{1,18,20,30-32} Cervical swabs contained a small population of HLA-G+ and CK7+ cells (Figures 2C and 2D, S1B) where only $1.88 \pm 1.45\%$ of cervical swabs cells were HLA-G+ and $1.04 \pm 0.96\%$ CK7+ cells. Blood cells often hampered generating a single cell suspension by promoting cellular clumping. To enrich trophoblast cells, we performed a density gradient and CD45+ blood cell depletion (Figure 2E). The top layer of the gradient was expected to correspond to reported densities of trophoblast cells, enabling their preferential enrichment during the separation process. Indeed, panCK+ and CK7+ cells were highly enriched in top fraction and absent in the middle and lower fractions (Figures 2F and S1C). Immunofluorescence quantification showed a significant enrichment of CK7+ cells in comparison to bulk cellular populations, reaching $12.67 \pm 4.42\%$ of enriched transcervical swab samples (Figures 2G and S1D). Fewer HLA-G+ cells were

(F) Heatmap of differentially expressed genes (DEGs) between transcervical clusters. Colors indicate relative expression.

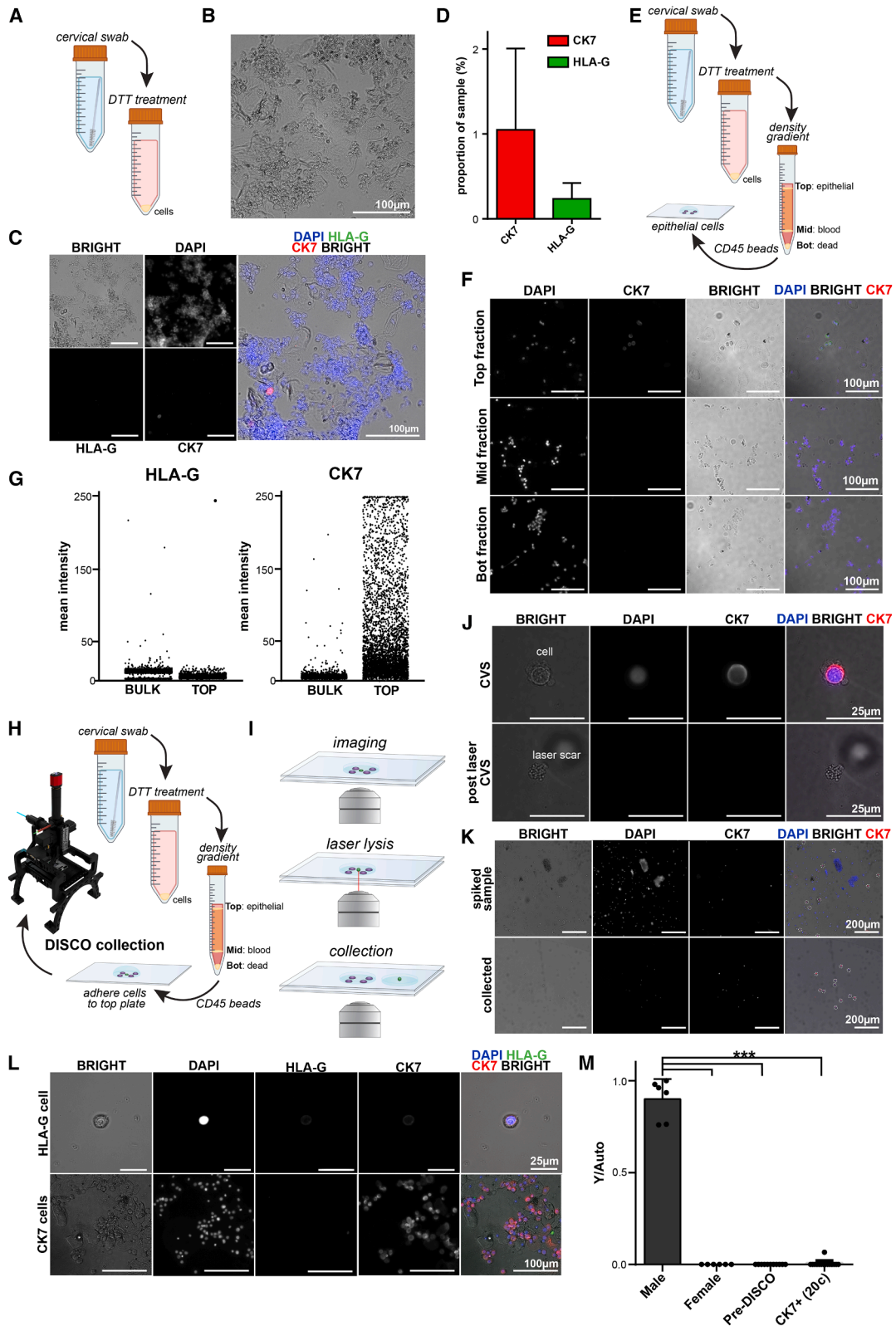
(G) UMAP of cervical swab cells labeled by gestational age.

(H) UMAP plots from (E) showing normalized log expression of indicated genes.

(I) UMAP plot of only epithelial cervical clusters.

(J) Diffusion map of epithelial cervical cells.

(K) UMAP plots from (I) showing normalized log expression of indicated genes.



(legend on next page)

identified in the top cellular fraction, suggesting many of the previously identified HLA-G+ cells may not be of trophoblast origin.

CK7+ and HLA-G are insufficient to identify fetal cells from cervical swabs

To isolate prospective CK7+ or HLA-G+ fetal cells from cervical swab cell suspensions, we utilized digital microfluidic isolation of single cells for omics (DISCO) (Figure 2H). This DISCO platform integrates fluorescence microscopy, with laser collection, and digital microfluidics, enabling the precise identification and collection of cells with a particular protein profile. Collected cells from cervical swabs were successfully adhered and integrated in the DISCO platform.

Only a very small fraction of CK7+ or HLA-G+ cells were identified in transcervical swab samples (Figures 2G and S1E). To determine if our DISCO platform could identify and collect prospective fetal cells, we spiked cells obtained from chorionic villus sampling (CVS) into bulk cervical swab samples at known proportions (Figure S1F). The outer layer of chorionic villus samples represents placental cytotrophoblast and shares many molecular markers with other placental cell types. We identified 98% of the expected proportion of CVS cells at concentrations ranging from 0.5% to 8% (Figures S1F and S1G). To determine the specificity of DISCO laser collection, we collected CVS cells from spiked bulk samples (Figure 2I). CVS cells were successfully collected by laser collection as identified by CK7+ and measuring less than 20 μm in diameter, demonstrating that single CVS cells could be specifically collected (Figures 2J and 2K). Collected samples showed no loss of lysed CK7+ CVS cells and no extraneously collected CK7- maternal cells (Figure 2K). All collected cells had intact DAPI signal, suggesting that nuclear DNA was robustly collected by the digital microfluidic system. Thus, we showed that our DISCO platform is able to identify small subpopulations of cells by immunofluorescent analysis and collect them with high accuracy.

To identify if collected cells were fetal, a positive fetal DNA profile was required for comparison. Consequently, pure fetal DNA was extracted from matched placental samples for each cervical swab. For ease of identification, we focused on male fetal samples which contained a Y chromosome that was easily detected

by PCR. Utilizing our DISCO platform, CK7+ and HLA-G+ cells from male fetuses were collected as groups of 1–5 cell (Figure 2L). To achieve the DNA concentration required for downstream sequencing, we performed whole-genome amplification (WGA) on the collected cell groups. Whole genome sequencing of WGA amplified samples demonstrated coverage on all chromosomes from a single cell, supporting the high-quality DNA obtained from cervical swab cells (Figure S1I). Revealingly, most HLA-G+ and CK7+ cells did not contain a Y chromosome, suggesting collected cells were not fetal in origin (Figure S1H). To determine if fetal DNA was detectable in larger groups of CK7+ cells, we collected groups of twenty CK7+ cells of varying morphologies. Fetal DNA was only detected in $15.96 \pm 3.78\%$ of grouped CK7+ samples (Figure 2M). Y chromosome/autosomal chromosome ratios averaged 0.00386 ± 0.00264 , suggesting an extremely small fetal DNA fraction within CK7+ twenty cell groups (Figure 2M). Thus, HLA-G and CK7 alone do not appear suitable for reliably identifying fetal cells in cervical swab samples.

Identification of a fetal cell profile from single cell RNA sequencing of placenta

To generate a reference for identifying potential fetal cells in transcervical swabs, we performed 10x single-cell RNA sequencing on placental tissues collected after elective termination from the corresponding donors. 7.6 weeks placenta was sequenced, yielding 9,511 sequenced cells (Figure 3A). The functional units of mid first trimester placenta are placental villi, which are composed of an outer layer of trophoblast surrounding an inner core of stroma and blood vessels. Multidimensional reduction and cellular cluster annotations using known marker genes revealed the expected cell types at week 7, including endothelial cells, stroma, blood cells, and trophoblasts (Figures 3A and 3B). Inner tissue types such as stroma, blood cell, and endothelial cell populations were also identified, indicating complete dissociation of the placental structure (Figures 3A and 3B). Trophoblasts are guaranteed to be fetal in origin, in contrast to stromal, endothelial, or most blood cells. Trophoblast subtypes syncytiotrophoblast (CGB3) and extravillous trophoblast (EVT) (HLA-G) were detectable with the

Figure 2. Transcervical swabs contain HLA-G and CK7 positive cells

- (A) Schematic of cervical swab mucolytics.
(B) Brightfield image of dissociated endocervical swab.
(C) Immunofluorescence staining (IF) of transcervical swab samples.
(D) Quantification of HLA-G and CK7 signal in endocervical swab IF. $n = 4$.
(E) Schematic of epithelial cell enrichment.
(F) IF of density gradient fractions (TOP, epithelial; MID, blood) and unfractionated cells (BULK).
(G) Quantification of HLA-G and CK7 signal in endocervical swab top and bulk fractions. $n = 4$ (cervical samples).
(H) Schematic of loading endocervical swabs cells into DISCO platform.
(I) Schematic of DISCO laser collection.
(J and K) IF of (J) CVS cell before and after laser collection and (K) after digital microfluidic collection.
(L) IF of DISCO targeted CK7+ or HLA-G+ cells in endocervical swabs.
(M) Plot of qPCR analysis of Y chromosome to autosomal chromosome ratios in indicated samples. Y/Auto: Y chromosome/autosomal chromosome. Male, male control genomic DNA $n = 6$; female, female controls genomic DNA $n = 6$; pre-disco, enriched endocervical swab sample $n = 10$; CK7+ (20c), 20 cell group of CK7+ cells from endocervical swabs $n = 19$. n represents independently collected cell groups unless specified. Error bars represent mean \pm SD and difference was determined using a two-tailed t test (* $p < 0.05$, ** $p < 0.01$, *** $p < 0.001$). Scale bars are indicated in each figure. Background intensity was equalized between channels to normalize for hydrophilic spot background.

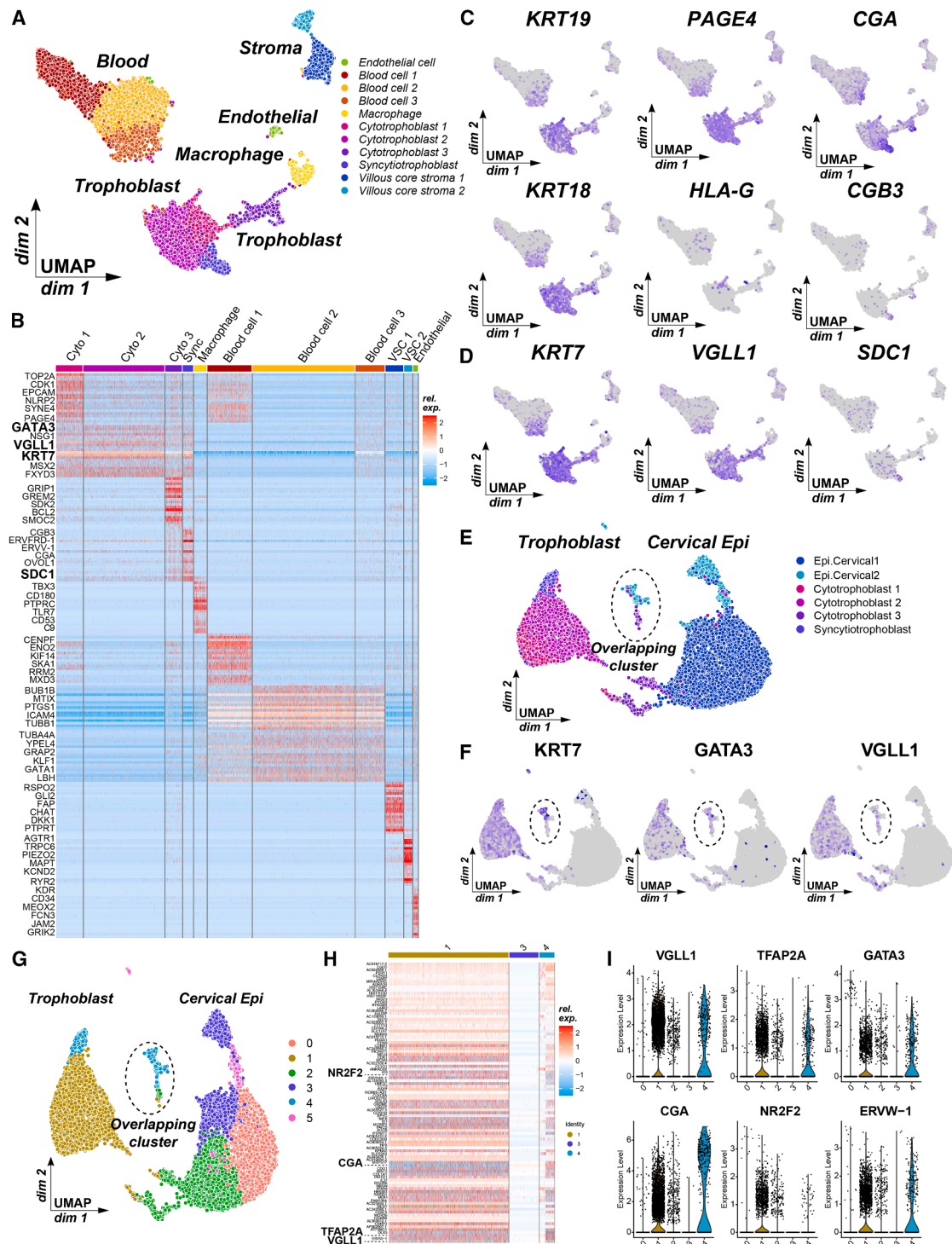


Figure 3. Identification of a fetal cell profile from single cell RNA sequencing of placenta

(A) UMAP plot of 10x RNA sequenced placental cells.
 (B) Heatmap of DEGs between placental clusters. Colors indicate relative expression.
 (C and D) UMAP plots from (A) showing normalized log expression of trophoblast genes.
 (E) UMAP plot of hierarchical clustering of transcervical swab cervical epithelium and trophoblast subpopulations.
 (F) UMAP plots from (E) showing normalized log expression of indicated genes.
 (G) UMAP plot of unbiased hierarchical clustering of (E).

(legend continued on next page)

trophoblast cluster (Figure 3C). Identified trophoblast subclusters expressed known trophoblast markers such as KRT7, GATA3, SDC1, and VGLL1 (Figures 3C and 3D). Notably, few HLA-G+ EVT were observed, likely due to their migration into the uterine lining.

To identify prospective trophoblast cells in our cervical swab dataset, we merged and renormalized our trophoblast placental dataset with the cervical epithelia clusters from our cervical swab dataset (Figure 3E). Interestingly, a central group of cells contained contributions from both the cervical epi 2 swab cluster and placental cytotrophoblast cluster (Figure 3E). This central group was enriched for trophoblast specific markers such as GATA3, and VGLL1 (Figure 3F). To determine which trophoblast subpopulations may be present in transcervical swabs, we performed hierarchical clustering on the merged placenta-cervical epithelium dataset. We identified cluster 4 as containing cells from the cytotrophoblast, syncytiotrophoblast, and a small subset of cells from transcervical swabs (Figure 3G), suggesting cytotrophoblast and syncytiotrophoblast cells may be present in cervical swabs. Isolating the transcervical swab cells within cluster 4 revealed 154 potential fetal cells across all gestational ages, amounting to 0.437% of transcervical swab cells.

Previous results showed enrichment of the trophoblast marker KRT7 in the cervical epithelium (Figure 1H). DISCO collection of CK7+ transcervical swab cells yielded predominantly maternal DNA, suggesting CK7 is found in maternal cell populations. To identify a fetal cell marker profile specific to transcervical swabs, we performed differential expression analysis between cluster 4 (combined cluster containing placenta and cervical swab cells) and cluster 1 (composed of predominantly cervical epithelium). DEGs were further trimmed by retaining only genes identified as highly expressed in placental cells in Figure 3H. A marker panel of 147 genes was ultimately identified, including known placental markers such as TFAP2A and VGLL1 (Figures 3H and 3I). Utilizing this panel, we found 0.02% of transcervical swab cells were highly enriched for our fetal cell marker panel, suggesting fetal cells are a rare population within transcervical swabs. Thus, we have generated a fetal cell marker panel and identified a small subpopulation of potential fetal cells in transcervical swabs.

Fetal DNA can be collected from endocervical swabs via DISCO

To ensure our fetal cell marker panel is expressed at the protein level in fetal placenta, we performed immunofluorescent staining of placental samples from 5 to 10 weeks of gestation. Findings show enrichment of trophoblast markers at both stages of placental development (Figure 4A), suggesting that our fetal cell marker set is effective in cervical swab samples at least from 5 to 10 weeks of gestation. We identified VGLL1 and TFAP2A in tandem with CK7 to be preferential markers due to their expression in the placental trophoblast and availability of robust antibodies. We identified small populations of CK7+ VGLL1+ or CK7+ TFAP2A + cells in transcervical swabs

(Figure 4B). However, the wide range of observed morphologies and cell sizes suggested that these marker profiles were still capturing multiple cell populations. (Figure 4C). Utilizing our DISCO platform, we collected a variety of CK7+ VGLL1+ cells (Figure 4D). Male fetal samples were selected to enable identification of fetal DNA via PCR for loci on the Y chromosome. We were able to detect fetal DNA in ~50% of single cells from three cervical swab samples, each comprising six individually collected cells (Figure 4E).

Cryo-sectioned *in vivo* placental cytotrophoblast and CVS samples exhibit cellular diameters ranging from 10 to 15 μm (Figure S2A). Notably, a majority of CK7+ vaginal and cervical epithelial cells in transcervical swabs had diameters larger than 20 μm , suggesting that most of CK7+ cells in transcervical swabs are maternal in origin (Figure 4F). Utilizing these criteria, we performed image analysis of enriched transcervical swabs and determined <20 μm CK7+ VGLL1+ constituted 0.09% of enriched fetal swab samples, while <20 μm CK7+ TFAP2A + cells made up 0.16% of enriched samples. Thus, to identify potential fetal cells in cervical swabs and exclude larger maternal cells, we selected cells that expressed VGLL1, GATA3, or TFAP2A in combination with CK7 that were less than 20 μm in diameter.

Collections of small pools of <20 μm CK7+ VGLL1+ single cells (5 cells per pool) contained detectable Y chromosome DNA in 80.0% of cases ($n = 15$) (Figure 4G). 73.3% of CK7+ TFAP2A + five cell pools contained fetal DNA ($n = 15$) (Figure 4G). However, quantitative PCR for fetal DNA showed a much lower proportion of Y chromosome DNA compared to male placental cells, suggesting our samples still contained contaminating maternal DNA (Figure 4H). To assess if DNA from collected cervical swab cells is suitable for diagnostics, we performed whole genome sequencing of four prospective fetal samples each consisting of five isolated cells. We were able to identify DNA from all chromosomes, including coverage on the Y chromosome (Figure S2B). However, variability in coverage across the genome hampered more in-depth analyses, likely as a consequence of whole genome amplification bias (Figure S2B).

Cell-free DNA (cfDNA), predominantly maternal in origin, can adhere to the surface of isolated fetal cells or the surfaces of our microfluidic device and be co-extracted during DNA isolation. cfDNA fragments can range in size but are typically under 200 bp. To characterize the size distribution of contaminating maternal DNA, we performed PowerQuant qPCR analysis on CK7+ cells, and CK7+ VGLL1+ cells, which utilizes matched primer pairs targeting short (89 bp) and long (294 bp) amplicons. CK7+ and CK7+ VGLL1+ samples contained a higher proportion of short DNA fragments compared with genomic controls, suggesting cfDNA contamination.

To further minimize potential cfDNA contamination, we performed nuclear isolation of transcervical swab samples via sonication. Immunofluorescent analysis of sonicated samples revealed numerous free nuclei (Figure S2C). Free nuclei expressing the nuclear-localized fetal cell marker VGLL1 were collected (Figure 4J) and found to contain detectable Y

(H) Heatmap of fetal cell marker panel in select clusters from (G), featuring cluster 1 (yellow, predominantly placental trophoblast), cluster 3 (purple, predominantly cervical epithelium), and cluster 4 (turquoise, overlapping cluster of placental trophoblast and transcervical swab cells).

(I) Violin plots of normalized expression of select fetal cell marker genes in merged transcervical swab—placental trophoblast dataset from (G and H).

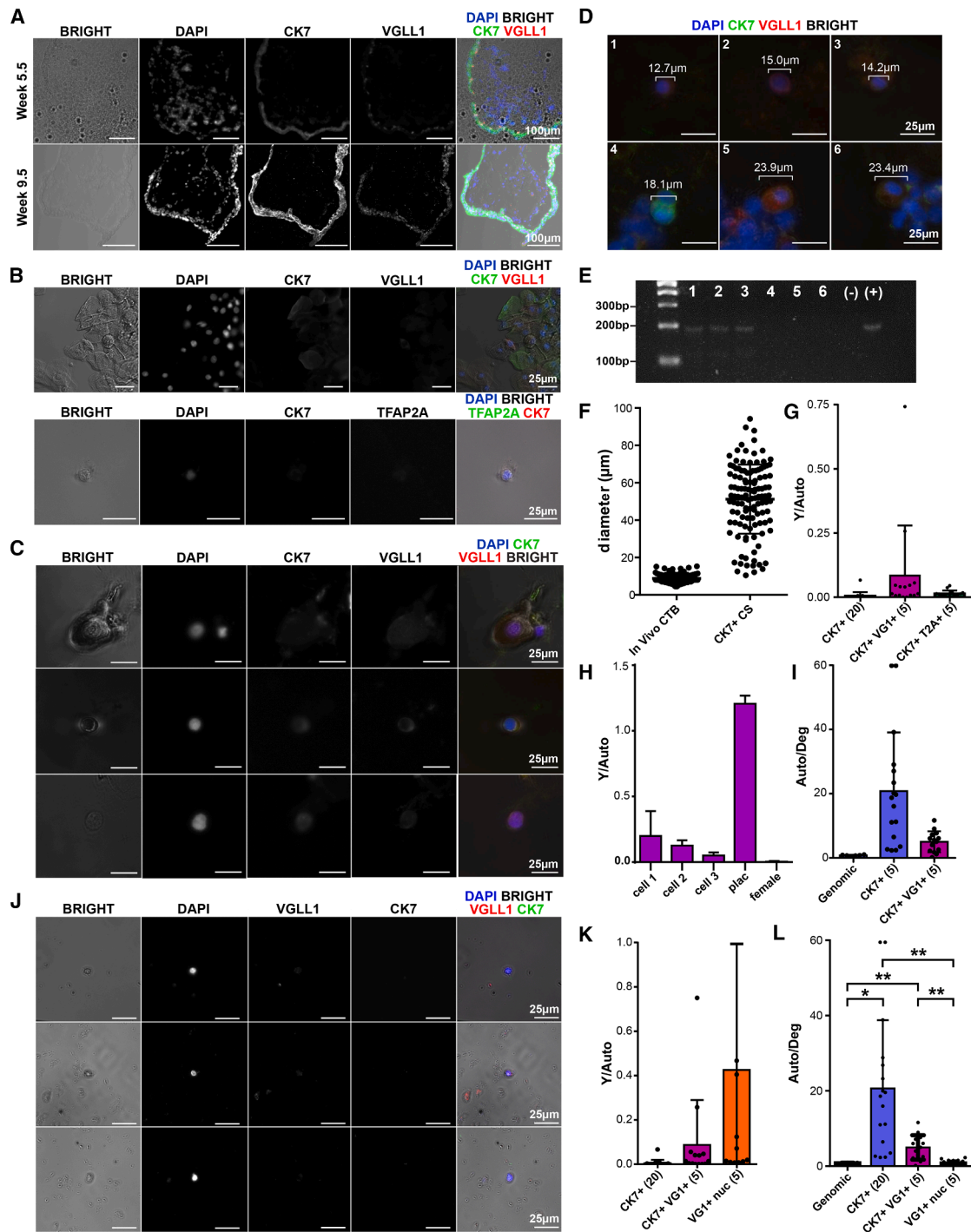


Figure 4. Fetal DNA can be collected from transcervical swabs via DISCO

(A) IF of week 5 and week 9 placenta for fetal cell markers.

(B–D) IF of potential fetal cells from transcervical swabs for indicated marker proteins. Cellular diameters are displayed in (D) for each cell.

(E) Electrophoretic gel of Y chromosome PCR of VGLL1 + /CK7 + cells from transcervical swabs. Collected cells: numbered lanes 1–6 associated with DISCO collected cells from transcervical swabs in (D) (+), male control DNA; (–), female control DNA. *n* = 6.

(F) Quantification of the diameter of in vivo placental cytotrophoblast and CK7 + transcervical swab cells (120 cells each). Ladder sizes are indicated on the gel. *n* = 4 (cervical samples).

(legend continued on next page)

chromosome DNA (Figure 4K). Notably, whole genome amplified nuclear fetal samples showed a significant reduction in relative short fragment DNA (Figure 4L), suggesting that majority of fragmented DNA was adhered to the plasma membrane. However, maternal DNA contamination persisted in amplified fetal samples as indicated by the persisting variability and lower abundance of Y chromosome amplicons (Figure 4K).

Although SNP analysis can be influenced by copy number variation through dosage effects, it remains a robust approach for identifying disease-associated variants. As a proof of concept, we amplified and sequenced 71 highly polymorphic, non-disease-associated regions from small pools (1–5 cells) of putative fetal cells, fetal placenta, and maternal cervical samples to assess SNP differences between fetus and mother. Thirty-five SNPs exhibited differential alleles between maternal and fetal DNA (Figure S2D). Despite variability in fetal allelic ratios, fetal specific genotypes were detectable in $55.7 \pm 8.2\%$ of prospective fetal samples from transcervical swabs (Figure S3), with 52.9% of detected genotypes being identified in all replicates (Figure S3). These findings support the potential of cervical swab-derived fetal DNA for disease-relevant genetic analysis.

DISCUSSION

In this study, we set out to isolate fetal cells from transcervical samples collected in early pregnancy using a previously validated microfluidic platform (DISCO) designed for rare cell capture. Our approach was guided by prior reports describing the use of CK7 and HLA-G as the gold standard markers for identifying EVT, including cell picking strategies and the well-established trophoblast retrieval and isolation from the cervix (TRIC) protocol.^{17,27,30,33}

Through iterative optimization, we developed a protocol to generate fetal cell enriched single-cell suspensions from transcervical swabs compatible with our microfluidic system for the collection of putative fetal cells. Disappointingly, samples enriched for CK7⁺ and HLA-G⁺ cells were either entirely maternal or contained only a minimal admixture of fetal DNA, insufficient for downstream genetic analysis. Our DISCO platform enabled the isolation of CK7⁺ or HLA-G⁺ transcervical swab cells from enriched cell suspensions. Yet, the continued absence of Y chromosome sequences indicated that the collected cells were not of fetal origin, raising concerns about the true cellular composition of the transcervical samples, and whether CK7 and HLA-G alone were sufficient for reliably identifying fetal cells in this context.

These concerns prompted us to undertake an unbiased molecular profiling of transcervical samples, an approach not previ-

ously applied in this setting, to gain deeper insight into the cellular landscape of transcervical brushings in early pregnancy. The HLA-G marker was largely confined to blood cells, limiting its utility for fetal cell identification on its own. A subset of keratin expressing cells emerged within the cervical epithelium cluster, which did not segregate by gestational age. However, while these markers have been effectively used to identify circulating trophoblast in maternal blood,²⁰ many of these genes have been reported to be expressed in cervical and vaginal epithelium.^{34,35}

Integration of matched fetal placental transcriptomes enabled the generation of a fetal cell marker panel, which included keratins as well as TFAP2A and VGLL1. Furthermore, placental trophoblasts typically ranged between 5 and 20 μm in diameter, excluding larger syncytiotrophoblast lining the placental villi. Interestingly, few HLA-G positive EVT were identified in our transcervical swabs. We hypothesize the lack of a distinct EVT cluster from our placental dataset resulted in transcervical swab EVT clustering with other trophoblast subpopulations. DISCO isolation experiments using a male sample demonstrated that cells under 20 μm in size with high VGLL1 and TFAP2A expression were positive for Y chromosome DNA, confirming their fetal origin. Incorporating cell size and with molecular profiles will enable AI-powered cell segmentation software to fully automate fetal cell isolation.

The selection criteria proposed in this study was derived from overlapping molecular profiles between transcervical swabs and placental cytotrophoblast. Cell size cutoffs below 20 μm likely excluded other fetal trophoblast cell types such as syncytiotrophoblasts. Previous NIPT studies have identified EVT and syncytiotrophoblasts in transcervical swabs samples^{31,36} and utilized other trophoblast markers such as HLA-G and $\beta\text{-HCG}$. However, the paucity of identified HLA-G⁺ EVT or syncytiotrophoblast populations in transcervical swabs as determined by single cell sequencing further substantiates the need for targeted cell collections strategies. Future studies will focus on developing additional selection criteria to capture a broader range of trophoblast subtypes for subsequent DISCO collection and pooling for downstream DNA analysis.

However, despite the refinement of our selection parameters, genomic sequencing results revealed an admixture of maternal and highly fragmented DNA. The consistent presence of maternal DNA in isolated cell samples suggests that contamination may stem from extracellular, cell-free maternal DNA rather than inadvertent capture of maternal cells. cfDNA—predominantly maternal in origin—can adhere to the surface of isolated fetal cells or the surfaces of our microfluidic device and be

(G and H) Plot of Y chromosome qPCR of DISCO collected groups of cells. Y/Auto: Y chromosome/autosomal chromosome. (G) CK7 + (20), 20 cell groups of CK7 + cells $n = 18$. CK7 + VG1 + (5), five cell groups of CK7 + VGLL1 + cells $n = 15$. CK7 + T2A + (5), five cell groups of CK7 + TFAP2A + cells, $n = 15$. (H) VGLL1 + CK7 + cells from endocervical swabs. $n = 3$ (technical replicates).

(I) Plot of degradation qPCR of indicated samples. Auto/Deg: short autosomal chromosome (89 bp)/long degradation chromosome (294 bp). Genomic, control genomic extract.

(J) IF of DISCO collected endocervical swab nuclei expressing nuclear fetal markers.

(K and L) Plot of (K) Y chromosome and (L) degradation qPCR of DISCO collected groups of cells and nuclei. VG1 + nuc (5), five cell groups of VGLL1 + nuclei, $n = 15$. Error bars represent mean + SD and difference was determined using a two-tailed t test (* $p < 0.05$, ** $p < 0.01$, *** $p < 0.001$). n represents independently collected cell groups unless specified. Scale bars are indicated in each figure. Background intensity was equalized between channels to normalize for hydrophilic spot background.

co-extracted during DNA isolation. Analysis of contaminating maternal DNA demonstrated a combination of long and short DNA fragments, suggesting contributions from both short cfDNA and larger genomic contaminant in collected fetal samples. Nuclear isolation greatly reduced short cfDNA contamination in fetal samples but did not fully eliminate maternal DNA. We hypothesize that larger maternal DNA fragments arise from lysed maternal cells during sample processing and nuclear isolation rather than from the *in vivo* uterine environment.

55.7 ± 8.2% of fetal SNPs were detectable in DISCO collected samples, 52.9% of which were consistently identified across all replicates. Interestingly, 8 SNPs showed consistent maternal signal, suggesting some primer pairs preferentially amplified maternal DNA. Variance in fetal allelic ratios is likely compounded by differences in region-specific maternal contamination and amplification bias across genomic regions. Whole genome amplification can exacerbate contamination by preferentially amplifying external, fragmented, and easily accessible DNA, complicating analyses dependent on genomic copy number and potentially masking fetal DNA signatures. Moreover, allelic dropout has been reported in low cell number samples subjected to WGA.³⁷ Developing panels to detect fetal variants for diagnostic use will require careful optimization of primer efficiency and reducing maternal DNA contamination. This highlights a critical technical barrier and underscores the need for improved purification strategies to enhance the specificity and reliability of cbNIPT and potentially uncover fetal cell populations that may otherwise be missed. Future studies will focus on developing novel methods to perform nuclear fractionation on DISCO to optimize nuclear isolation and minimize DNA contamination. Thus, our study highlights the need for better markers, improved cell characterization strategies, and perhaps novel approaches to overcome these biological and technical hurdles. Despite decades of effort and notable technological advances, cbNIPT remains an elusive goal.

Limitations of the study

A limitation to this study is the lack of incorporation of cell morphological features into the selection strategy. Integrating morphological assessment could have provided an additional layer of discrimination and allow for automated cell collection. Expanding fetal cell selection criteria will enable the collection of a greater variety of fetal cell types. Future studies will combine molecular markers with quantitative morphological criteria to ultimately achieve more precise identification and capture large numbers of true fetal cells.

RESOURCE AVAILABILITY

Lead contact

Requests for further information and resources should be directed to and will be fulfilled by the lead contact, Elena Greenfeld (elena.greenfeld@sinaihealth.ca).

Materials availability

This study did not generate new unique reagents.

Data and code availability

- RNA sequencing data have been deposited at ArrayExpress and are publicly available as of the date of publication. Accession number,

E-MTAB-15846, <https://www.ebi.ac.uk/biostudies/ArrayExpress/studies/E-MTAB-15846?key=d333677d-0aa8-44cb-8125-b8e11ac9271f>.

- Scripts utilized in marker panel generation and analysis are available online: <https://github.com/DylanSiriwardena/DISCOdiagnostics>. Any additional information required to reanalyze the data reported in this study is available from the [lead contact](#) upon request.

ACKNOWLEDGMENTS

We are grateful to Mount Sinai services for their continued support of transcervical swab sample preparation, administration, and molecular profiling. We thank the Donnelly Sequencing Centre and Princess Margaret Genomics center for their support with whole genome sequencing and 10x RNA sequencing respectively. We thank Leticia Bodo for their assistance with running qPCR samples. This research was generously supported by a Disruptive Innovations in Genomics Grant from Genome Canada and the Ontario Genomics Institute. D.S. was supported by an Ontario Genomics and CIHR postdoctoral fellowship. A.R.W. also thanks the Canadian Foundation for Innovation and the Province of Ontario (36661) and the Canada Research Chairs Program (950-231616).

AUTHOR CONTRIBUTIONS

M.D.C., M.D.M.D., D.C., E.G., and A.R.W. conceptualized the project. D.S., M.D.C., M.D.M.D., D.C., C.T., J.L., F.A., S.G., and L.D. conducted experiments. D.S., M.D.C., D.C., C.T., J.L., F.A., and L.D. performed transcervical swab processing, DISCO device manufacture, and DISCO collection. D.S. performed single cell RNA sequencing, whole genome sequencing, SNP sequencing sample preparation. D.S. and C.T. performed PCR, placental dissection, sectioning, immunofluorescence staining, confocal microscopy, and image quantification. D.S., C.T., and M.D.M.D. performed RNA, whole genome, and SNP sequencing analysis. D.S. and S.G. performed qPCR analysis. D.S. and E.G. prepared the manuscript. D.C., E.G., and A.R.W. acquired funding and supervised the project.

DECLARATION OF INTERESTS

M.D.M.D., M.D.C., J.L., and A.R.W. are co-inventors on a related patent for the DISCO technology: US12364982B2 System for identifying and targeting individual cells within a heterogeneous population for selective extraction of cellular content.

STAR★METHODS

Detailed methods are provided in the online version of this paper and include the following:

- **KEY RESOURCES TABLE**
- **EXPERIMENTAL MODEL AND STUDY PARTICIPANT DETAILS**
 - Transcervical swabs
 - CVS cell collection
- **METHOD DETAILS**
 - Transcervical swab processing
 - Nuclear isolation
 - Placental embedding and cryosectioning
 - DISCO device manufacture, assembly, and operation
 - Cell adhesion and immunofluorescence
 - Cell collection
 - DNA purification
 - Whole genome amplification and PCR
 - Library preparation, SNP sequencing and nanopore sequencing
 - Samples and library preparation for 10x RNA sequencing
- **QUANTIFICATION AND STATISTICAL ANALYSIS**
 - 10x RNA sequencing analysis
 - Fetal cell panel generation
 - Image analysis
 - qPCR analysis

SUPPLEMENTAL INFORMATION

Supplemental information can be found online at <https://doi.org/10.1016/j.isci.2026.116413>.

Received: November 19, 2025

Revised: February 27, 2026

Accepted: May 29, 2026

REFERENCES

- Chiu, R.W.K., and Lo, Y.M.D. (2012). Noninvasive prenatal diagnosis empowered by high-throughput sequencing. *Prenat. Diagn.* 32, 401–406. <https://doi.org/10.1002/PD.3822>.
- Benn, P., Borrell, A., Cuckle, H., Dugoff, L., Gross, S., Johnson, J.A., Maymon, R., Odibo, A., Schieler, P., Spencer, K., et al. (2012). Prenatal Detection of Down Syndrome using Massively Parallel Sequencing (MPS): a rapid response statement from a committee on behalf of the Board of the International Society for Prenatal Diagnosis, 24 October 2011. *Prenat. Diagn.* 32, 1–2. <https://doi.org/10.1002/PD.2919>.
- Norton, M.E., Jacobsson, B., Swamy, G.K., Laurent, L.C., Ranzini, A.C., Brar, H., Tomlinson, M.W., Pereira, L., Spitz, J.L., Hollemon, D., et al. (2015). Cell-free DNA Analysis for Noninvasive Examination of Trisomy. *N. Engl. J. Med. Overseas. Ed.* 372, 1589–1597. https://doi.org/10.1056/NEJMOA1407349/SUPPL_FILE/NEJMOA1407349_DISCLOSURES.PDF.
- Lo, Y.M.D., Corbetta, N., Chamberlain, P.F., Rai, V., Sargent, I.L., Redman, C.W., and Wainscoat, J.S. (1997). Presence of fetal DNA in maternal plasma and serum. *Lancet* 350, 485–487. [https://doi.org/10.1016/S0140-6736\(97\)02174-0](https://doi.org/10.1016/S0140-6736(97)02174-0).
- Palomaki, G.E., Kloza, E.M., Lambert-Messerlian, G.M., Haddow, J.E., Neveux, L.M., Ehrich, M., Van Den Boom, D., Bombard, A.T., Decui, C., Grody, W.W., et al. (2011). DNA sequencing of maternal plasma to detect Down syndrome: An international clinical validation study. *Genet. Med.* 13, 913–920. <https://doi.org/10.1097/GIM.0b013e3182368a0e>.
- Ashoor, G., Syngelaki, A., Poon, L.C.Y., Rezende, J.C., and Nicolaidis, K.H. (2013). Fetal fraction in maternal plasma cell-free DNA at 11–13 weeks' gestation: relation to maternal and fetal characteristics. *Ultrasound Obstet. Gynecol.* 41, 26–32. <https://doi.org/10.1002/UOG.12331>.
- Canick, J.A., Palomaki, G.E., Kloza, E.M., Lambert-Messerlian, G.M., and Haddow, J.E. (2013). The impact of maternal plasma DNA fetal fraction on next generation sequencing tests for common fetal aneuploidies. *Prenat. Diagn.* 33, 667–674. <https://doi.org/10.1002/PD.4126>.
- Hui, L., and Bianchi, D.W. (2019). Fetal fraction and noninvasive prenatal testing: What clinicians need to know. *Prenat. Diagn.* 40, 155–163. <https://doi.org/10.1002/PD.5620>.
- Sun, K., Jiang, P., Wong, A.I.C., Cheng, Y.K.Y., Cheng, S.H., Zhang, H., Chan, K.C.A., Leung, T.Y., Chiu, R.W.K., and Lo, Y.M.D. (2018). Size-tagged preferred ends in maternal plasma DNA shed light on the production mechanism and show utility in noninvasive prenatal testing. *Proc. Natl. Acad. Sci. USA* 115, E5106–E5114. <https://doi.org/10.1073/PNAS.1804134115;WEBSITE:WEBSITE:PNAS-SITE;WGROU:STRING:PUBLICATION>.
- Lo, Y.M.D., Chan, K.C.A., Sun, H., Chen, E.Z., Jiang, P., Lun, F.M.F., Zheng, Y.W., Leung, T.Y., Lau, T.K., Cantor, C.R., and Chiu, R.W.K. (2010). Maternal plasma DNA sequencing reveals the genome-wide genetic and mutational profile of the fetus. *Sci. Transl. Med.* 2, 61ra91. <https://doi.org/10.1126/SCITRANSLMED.3001720>.
- Pan, M., Chen, P., Lu, J., Liu, Z., Jia, E., and Ge, Q. (2020). The fragmentation patterns of maternal plasma cell-free DNA and its applications in non-invasive prenatal testing. *Prenat. Diagn.* 40, 911–917. <https://doi.org/10.1002/PD.5680;WGROU:STRING:PUBLICATION>.
- Benn, P., and Cuckle, H. (2014). Theoretical performance of non-invasive prenatal testing for chromosome imbalances using counting of cell-free DNA fragments in maternal plasma. *Prenat. Diagn.* 34, 778–783. <https://doi.org/10.1002/PD.4366>.
- Bussani, C., Cioni, R., Mattei, A., Fambrini, M., Marchionni, M., and Scarselli, G. (2007). Prenatal diagnosis of common aneuploidies in transcervical samples using quantitative fluorescent-PCR analysis. *Mol. Diagn. Ther.* 11, 117–121. <https://doi.org/10.1007/BF03256231>.
- Pfeifer, I., Benachi, A., Saker, A., Bonnefont, J.P., Mouawia, H., Broncy, L., Frydman, R., Brival, M.L., Lacour, B., Dachez, R., and Paterlini-Bréchet, P. (2016). Cervical trophoblasts for non-invasive single-cell genotyping and prenatal diagnosis. *Placenta* 37, 56–60. <https://doi.org/10.1016/j.placenta.2015.11.002>.
- Mantzaris, D., and Cram, D.S. (2015). Potential of syncytiotrophoblasts isolated from the cervical mucus for early non-invasive prenatal diagnosis: Evidence of a vanishing twin. *Clin. Chim. Acta* 438, 309–315. <https://doi.org/10.1016/j.cca.2014.09.002>.
- Bussani, C., Cioni, R., Scarselli, B., Barciulli, F., Bucciantini, S., Simi, P., Fogli, A., and Scarselli, G. (2002). Strategies for the isolation and detection of fetal cells in transcervical samples. *Prenat. Diagn.* 22, 1098–1101. <https://doi.org/10.1002/PD.469>.
- Katz-Jaffe, M.G., Mantzaris, D., and Cram, D.S. (2005). DNA identification of fetal cells isolated from cervical mucus: Potential for early non-invasive prenatal diagnosis. *BJOG* 112, 595–600. <https://doi.org/10.1111/J.1471-0528.2004.00506.X>.
- Jain, C.V., Kadam, L., Van Dijk, M., Kohan-Ghadr, H.R., Kilburn, B.A., Hartman, C., Mazzorana, V., Visser, A., Hertz, M., Bolnick, A.D., et al. (2016). Fetal genome profiling at 5 weeks of gestation after noninvasive isolation of trophoblast cells from the endocervical canal. *Sci. Transl. Med.* 8. https://doi.org/10.1126/SCITRANSLMED.AAH4661/SUPPL_FILE/8-363RE4_SM.PDF.
- Kang, H.G., Kim, S.H., Lim, J.H., Intisar, A., Yang, S., Kim, J.M., Kang, H.J., Shin, H.Y., Yang, S.J., Ryu, H.M., and Kim, M.S. (2023). Continuous centrifugal microfluidics identifies the marker and size heterogeneity of circulating trophoblasts for accurate non-invasive prenatal diagnosis. *Sens. Actuators B Chem.* 394, 134331. <https://doi.org/10.1016/J.SNB.2023.134331>.
- Doffini, A., Forcato, C., Mangano, C., Lattuada, D., Aversa, R., Maranta, C., Giovannone, E.D., Buson, G., Bolognesi, C., Maiocchi, R., et al. (2023). Isolation of single circulating trophoblasts from maternal circulation for noninvasive fetal copy number variant profiling. *Prenat. Diagn.* 43, 14–27. <https://doi.org/10.1002/PD.6275;WGROU:STRING:PUBLICATION>.
- Mohamed, H., Turner, J.N., and Caggana, M. (2007). Biochip for separating fetal cells from maternal circulation. *J. Chromatogr. A* 1162, 187–192. <https://doi.org/10.1016/j.chroma.2007.06.025>.
- Huang, R., Barber, T.A., Schmidt, M.A., Tompkins, R.G., Toner, M., Bianchi, D.W., Kapur, R., and Flejter, W.L. (2008). A microfluidics approach for the isolation of nucleated red blood cells (NRBCs) from the peripheral blood of pregnant women. *Prenat. Diagn.* 28, 892–899. <https://doi.org/10.1002/PD.2079>.
- Vossaert, L., Chakchouk, I., Zemet, R., and Van den Veyver, I.B. (2021). Overview and recent developments in cell-based noninvasive prenatal testing. *Prenat. Diagn.* 41, 1202–1214. <https://doi.org/10.1002/PD.5957>.
- Cayrefourcq, L., Vincent, M.C., Pierredon, S., Moutou, C., Imbert-Boutteille, M., Haquet, E., Puechberty, J., Willems, M., Liautard-Haag, C., Molinari, N., et al. (2020). Single Circulating Fetal Trophoblastic Cells Eligible for Non Invasive Prenatal Diagnosis: the Exception Rather than the Rule. *Sci. Rep.* 10, 9861. <https://doi.org/10.1038/s41598-020-66923-9>.
- Yang, X., Du, L., Li, Y., Liang, L., Ma, L., and Wang, S. (2023). Trophoblast retrieval from the cervical canal to predict abnormal pregnancy early in gestation: a pilot study. *BMC Pregnancy Childbirth* 23, 193. <https://doi.org/10.1186/S12884-023-05499-4/TABLES/2>.
- Moser, G., Drewlo, S., Huppertz, B., and Armant, D.R. (2018). Trophoblast retrieval and isolation from the cervix: origins of cervical trophoblasts and

- their potential value for risk assessment of ongoing pregnancies. *Hum. Reprod. Update* 24, 484–496. <https://doi.org/10.1093/HUMUPD/DMY008>.
27. Bailey-Hytholt, C.M., Sayeed, S., Kraus, M., Joseph, R., Shukla, A., and Tripathi, A. (2019). A Rapid Method for Label-Free Enrichment of Rare Trophoblast Cells from Cervical Samples. *Sci. Rep.* 9, 12115. <https://doi.org/10.1038/s41598-019-48346-3>.
 28. Lamanna, J., Scott, E.Y., Edwards, H.S., Chamberlain, M.D., Dryden, M.D.M., Peng, J., Mair, B., Lee, A., Chan, C., Sklavounos, A.A., et al. (2020). Digital microfluidic isolation of single cells for -Omics. *Nat. Commun.* 11, 5632. <https://doi.org/10.1038/s41467-020-19394-5>.
 29. Scott, E.Y., Safarian, N., Casasbuenas, D.L., Dryden, M., Tockovska, T., Ali, S., Peng, J., Daniele, E., Nie Xin Lim, I., Bang, K.W.A., et al. (2024). Integrating single-cell and spatially resolved transcriptomic strategies to survey the astrocyte response to stroke in male mice. *Nat. Commun.* 15, 1584. <https://doi.org/10.1038/s41467-024-45821-y>.
 30. Bolnick, J.M., Kilburn, B.A., Bajpayee, S., Reddy, N., Jeelani, R., Crone, B., Simmerman, N., Singh, M., Diamond, M.P., and Armant, D.R. (2014). Trophoblast retrieval and isolation from the cervix (TRIC) for noninvasive prenatal screening at 5 to 20 weeks of gestation. *Fertil. Steril.* 102, 135–142.e6. <https://doi.org/10.1016/j.fertnstert.2014.04.008>.
 31. van Dijk, M., Boussata, S., Janssen, D., Afink, G., Jebbink, J., van Maarle, M., Wortelboer, E., Kooper, A., and Pajkrt, E. (2022). Tricky TRIC: A replication study using trophoblast retrieval and isolation from the cervix to study genetic birth defects. *Prenat. Diagn.* 42, 1612–1621. <https://doi.org/10.1002/PD.6260>.
 32. Hou, S., Chen, J.F., Song, M., Zhu, Y., Jan, Y.J., Chen, S.H., Weng, T.H., Ling, D.A., Chen, S.F., Ro, T., et al. (2017). Imprinted NanoVelcro Microchips for Isolation and Characterization of Circulating Fetal Trophoblasts: Toward Noninvasive Prenatal Diagnostics. *ACS Nano* 11, 8167–8177. <https://doi.org/10.1021/ACS.NANO.7B03073>.
 33. Bulmer, J.N., Cioni, R., Bussani, C., Cirigliano, V., Sole, F., Costa, C., Garcia, P., and Adinolfi, M. (2003). HLA-G positive trophoblastic cells in transcervical samples and their isolation and analysis by laser microdissection and QF-PCR. *Prenat. Diagn.* 23, 34–39. <https://doi.org/10.1002/PD.511>.
 34. Schaller, G., Lengyel, E., Pantel, K., Hardt, W., and Mischke, D. (1993). Keratin expression reveals mosaic differentiation in vaginal epithelium. *Am. J. Obstet. Gynecol.* 169, 1603–1607. [https://doi.org/10.1016/0002-9378\(93\)90444-N](https://doi.org/10.1016/0002-9378(93)90444-N).
 35. Smedts, F., Ramaekers, F., Link, M., Lauerova, L., Troyanovsky, S., Schijf, C., and Vooijs, G.P. (1994). Detection of keratin subtypes in routinely processed cervical tissue: implications for tumour classification and the study of cervix cancer aetiology. *Virchows Arch.* 425, 145–155. <https://doi.org/10.1007/BF00230351/METRICS>.
 36. Adinolfi, M., and Sherlock, J. (2001). Fetal cells in transcervical samples at an early stage of gestation. *J. Hum. Genet.* 46, 99–104. <https://doi.org/10.1007/S100380170095>.
 37. Estévez-Gómez, N., Prieto, T., Tomás, L., Alvarino, P., Guillaumet-Adkins, A., Heyn, H., Prado-López, S., and Posada, D. (2025). Differential performance of strategies for single-cell whole-genome amplification. *Cell Rep. Methods* 5, 101025. <https://doi.org/10.1016/j.crmeth.2025.101025>.
 38. Butler, A., Hoffman, P., Smibert, P., Papalexi, E., and Satija, R. (2018). Integrating single-cell transcriptomic data across different conditions, technologies, and species analysis. *Nat. Biotechnol.* 36, 411–420. <https://doi.org/10.1038/nbt.4096>.
 39. Li, H., Handsaker, B., Wysoker, A., Fennell, T., Ruan, J., Homer, N., Marth, G., Abecasis, G., and Durbin, R. (2009). The Sequence Alignment/Map format and SAMtools. *Bioinformatics* 25, 2078–2079. <https://doi.org/10.1093/BIOINFORMATICS/BTP352>.
 40. Rodeck, C., Tutschek, B., Sherlock, J., and Kingdom, J. (1995). Methods for the transcervical collection of fetal cells during the first trimester of pregnancy. *Prenat. Diagn.* 15, 933–942. <https://doi.org/10.1002/PD.1970151008>.
 41. Li, H. (2018). Minimap2: pairwise alignment for nucleotide sequences. *Bioinformatics* 34, 3094–3100. <https://doi.org/10.1093/BIOINFORMATICS/BTY191>.
 42. Liao, Y., Smyth, G.K., and Shi, W. (2014). featureCounts: an efficient general purpose program for assigning sequence reads to genomic features. *Bioinformatics* 30, 923–930.
 43. Dobin, A., Davis, C.A., Schlesinger, F., Drenkow, J., Zaleski, C., Jha, S., Batut, P., Chaisson, M., and Gingeras, T.R. (2013). STAR: Ultrafast universal RNA-seq aligner. *Bioinformatics* 29, 15–21.
 44. Angerer, P., Haghverdi, L., Büttner, M., Theis, F.J., Marr, C., and Buettner, F. (2016). Destiny: Diffusion maps for large-scale single-cell data in R. *Bioinformatics* 32, 1241–1243. <https://doi.org/10.1093/bioinformatics/btv715>.
 45. Schindelin, J., Arganda-Carreras, I., Frise, E., Kaynig, V., Longair, M., Pietzsch, T., Preibisch, S., Rueden, C., Saalfeld, S., Schmid, B., et al. (2012). Fiji: An open-source platform for biological-image analysis. *Nat. Methods* 9, 676–682. <https://doi.org/10.1038/nmeth.2019>.

STAR★METHODS

KEY RESOURCES TABLE

REAGENT or RESOURCE	SOURCE	IDENTIFIER
Antibodies		
GATA3 (rabbit)	Cell signaling	5852T; RRID: AB_10835690
AP2 γ (rabbit)	Cell signaling	2320S; RRID: AB_2202287
AP2 α	Santa Cruz	sc-12726; RRID: AB_667767
VGLL1	Novus Bio	31921; RRID: AB_3278908
HLA-G	BD Pharm.	557577; RRID: AB_396753
CK7 (rabbit)	Abcam	Ab53123; RRID: AB_869896
CK7 (mouse)	Invitrogen	14-9005-82; RRID: AB_10669584
panCK	BioLegend	628601; RRID: AB_628601
CD163	Cell signaling	D6U1J; RRID: AB_3720265
CGA	R&D	MAB4169; RRID: AB_2079126
Alexa Fluor 488 donkey anti-mouse	Invitrogen	A11001; RRID: AB_2534069
Alexa Fluor 647 donkey anti-goat	Invitrogen	SAB4600352
DAPI	Sigma-Aldrich	
Biological samples		
Transcervical swabs and matched placental samples	Mount Sinai Services	This paper
Chorionic villus samples	Mount Sinai Services	This paper
Chemicals, peptides, and recombinant proteins		
Dithithreitol (DTT)	Bioshop	DTT001.5
Benzonase	Millepore	71205
OptiPrep	stem cell technologies	07820
CD45 beads	Invitrogen	11153D
optimum cutting temperature (O.C.T)	TissueTek	4583
Poly-L-Lysine	Sigma	P4832
borate buffer	Thermo	28341
IGEPAL30	Bioshop	NON999.500
donkey serum	Thermo	116-4101
Critical commercial assays		
Picopure extraction kit	Thermo	KIT0103
Repli-g single cell kit	Qiagen	150343
Qubit DNA quantification	Invitrogen	Q32854
DreamTaq Green PCR MasterMix 2X	Invitrogen	FERK1081
PowerQuant qPCR mix	Promega	PQ5008
V14 nanopore ligation sequencing kit	Oxford Nanopore Technologies	SQK-LSK114
Deposited data		
Single cell RNA sequencing of transcervical swabs and placenta	This paper	E-MTAB-15846, https://www.ebi.ac.uk/biostudies/ArrayExpress/studies/E-MTAB-15846?key=d333677d-0aa8-44cb-8125-b8e11ac9271f
Oligonucleotides		
5 chromosome PCR and SRY PCR primers found in Table S3	This paper	N/A
Software and algorithms		
ImageJ/Fiji	Schindelin et al., 2012	https://imagej.nih.gov/ij/

(Continued on next page)

Continued

REAGENT or RESOURCE	SOURCE	IDENTIFIER
R	https://www.R-project.org/	v4.4.2
IGV V2.16.2	https://data.broadinstitute.org/igv/projects/downloads/2.16/	N/A
Seurat v5.1.0	Butler et al. ³⁸ , 2018; Stuart et al., 2019	N/A
Samtools	Li et al. ³⁹	http://samtools.sourceforge.net/
Other		
Resource website for this publication	This paper	https://github.com/DylanSiriwardena/DISCOdiagnostics

EXPERIMENTAL MODEL AND STUDY PARTICIPANT DETAILS

Transcervical swabs

Cervical cytobrush samples were collected from patients prior to termination by the Morgentaler Clinic as described below from gestational ages 5 to 12 weeks. All of samples were used under Human Research Protocol #39574, which was reviewed and approved by the Mount Sinai REB. The method for collection of cervical samples was adopted from Rodeck et al.⁴⁰ Briefly, a Medscand Cytobrush Plus GT Endocervical Sampler (CooperSurgical) was inserted 2 cm into the cervix, rotated to trap the cervical mucus and withdrawn. The end of the brush was then placed into a container with ~25-40 mL PBS and labelled with a unique ID. Participant personal details (sex, gender, ancestry, race, ethnicity, and socioeconomic status) were not provided to researchers. The developmental stage of sequenced samples is indicated. The gestational age of every sample utilized during the development of our platform is included as [Table S1](#).

CVS cell collection

Chorionic villus specimens were manually dissected by Diagnostic Medical Genetics lab under a stereomicroscope to remove maternal decidua and blood contamination. Tissue was subjected to enzymatic digestion with trypsin-EDTA to detach cytotrophoblasts. CVS cells were washed 3x in PBS before being fixed dropwise in ice cold Methanol and Acetic acid (3:1).

METHOD DETAILS

Transcervical swab processing

Cytobrushes and PBS containing transcervical swab samples were transferred to a 50mL falcon tube and centrifuged at 300g for 10 minutes to collect any cells in the supernatant. PBS volume was adjusted to 25 mL and 25 mL of DMEM (Gibco) with dithiothreitol (DTT) (Bioshop: DTT001.5), sodium bicarbonate (Na₂CO₃) (Sigma) and Benzonase® (Millepore: 71205) was added to a final concentration of 10 mM DTT, 1 mM Na₂CO₃, and 28 mU Benzonase to remove mucus. Samples were placed on a variable speed rocker (BR2000-GM 2D rocker, VWR) for 30 minutes at 37°C. Samples were centrifuged at 300xg for 10 minutes to collect transcervical swabs in solution.

To enrich for intact trophoblast cells, an OptiPrep (stem cell technologies: 07820) density gradient composed of 1 mL of 1.16 g/mL, 6 mL of 1.067 g/ml OptiPrep, and DMEM was then centrifuged at 800xg for 25 minutes, with the acceleration and deceleration parameters set to 7 and 0, respectively. The top 1 mL of the resulting upper layer (fraction) was removed and washed with 10mL of PBS. Cells were pelleted for 10 minutes at 300xg and resuspended in 100 µL of 1:1 DMEM/PBS. 50 µL of CD45 beads (Invitrogen: 11153D) were washed in 1mL of DMEM/PBS1X (1:1) and resuspended with the 100µL of cells to remove blood cells. Suspension was incubated for 20 min at 4°C with agitation. Magnetic CD45 beads were pelleted and the supernatant containing the remaining transcervical swab cells was transferred to a 1.5mL tube and washed with 500 µL of PBS. Cells were pelleted at 300xg, 10min, 4°C and resuspended dropwise in ice cold methanol and acetic acid (3:1). Cellular suspensions were either immediately spotted onto a top plate for immunofluorescent staining or stored at -20 °C.

Nuclear isolation

Nuclear isolates were generated from processed transcervical swab samples post methanol fixation. Fixed cells were resuspended in nuclear isolation buffer (HEPES 20mM, KCl 10mM, MgCl₂ 2mM, EDTA 1mM) and sonicated for 3 cycles at 30% amplitude for 10s with 10s rest in between. Lysates were centrifuged at 500xg for 5 minutes and the supernatant discarded. Cellular pellets were resuspended in PBS to the desired concentration and spotted on a top plate. Cells were allowed to settle and adhere to the top plate for 15 minutes.

Placental embedding and cryosectioning

Placental tissue was collected from pregnancy termination. Individual placental villi were dissected away from connective tissue under brightfield microscopy. ~1 gram of placental tissue was resuspended in PBS for whole genome DNA analysis. Placental tissue for imaging were immediately cryopreserved *in toto* by submerging in optimum cutting temperature (O.C.T) compound (4583, TissueTek) and snap-freezing in liquid nitrogen to preserve DNA and RNA integrity. O.C.T. blocks were sectioned to a 11 μm thickness, adhered to glass slides (Superfrost Plus, Thermo Scientific), and stored at -80°C for future IF or DNA analysis.

DISCO device manufacture, assembly, and operation

DISCO devices were manufactured as previously described.^{28,29} Briefly, DISCO devices are comprised of a bottom plate containing a chromium electrode array and conductive top plate with hydrophilic spots for cellular adhesion. In short, DISCO bottom plates were fabricated in the University of Toronto Centre for Research and Application in fluidic technologies (CRAFT) device foundry, using transparent photomasks printed at 20,000 DPI (Pacific Arts and Designs Inc.). The bottom plates of DISCO devices bearing arrays of chromium electrodes coated with dielectric and hydrophobic layers were formed using methods similar to those described previously.²⁸ The design features an array of 80 roughly square actuation electrodes (2.2×2.2 mm ea.) interfaced with 8 rectangular reservoir electrodes. Each driving electrode is connected to a contact pad designed to interface with a custom pogo-pin connector on the instrument. After processing, bottom plates were sterilized using 70% ethanol, air dried, and stored until use.

DISCO device top plates, bearing hydrophilic cell culture sites, were formed from 3" \times 1" indium-tin oxide (ITO) coated glass substrates (Delta Technologies Ltd) by milling. Briefly, substrates were cleaned with acetone, isopropanol, DI water and dried with nitrogen gas. Substrates were spin-coated with Teflon-AF 1600 (1% w/w in Fluorinert FC40, 2000 RPM, 30 s) and baked in an oven (180°C , 30 min). Hydrophilic spots were generated by removing the Teflon from a 1.75 mm diameter spot using a CNC milling machine.

The DISCO instrument is based upon an upright modular microscope system (Applied Scientific Instrumentation [ASI], RAMM/MIM system), as described previously.²⁹ Cells were lysed using a frequency doubled (532 nm) Q-switched Nd:YAG laser (Quantel, Ultra 50) focused through a $\times 100$ objective (BoliOptics, NA = 0.8) onto the inner surface of a DISCO top plate (where cells are adhered).

Cell adhesion and immunofluorescence

Hydrophilic spots on ITO top plates were pretreated with 0.01% Poly-L-Lysine (P4832) in 1x borate buffer (Thermo: 28341) for 15 minutes. Spots were washed with distilled water and air dried. Cellular suspensions were diluted with methanol and spotted onto the hydrophilic spots on the top plate. Methanol suspensions were allowed to dry before being washed with PBS to remove non-adhered cells. Placental cryosections were fixed with 4% paraformaldehyde in PBS for 10 min at room temperature. Permeabilization was performed in 0.25% IGEPAL30 (Bioshop:NON999.500) in PBS (Thermo Fisher Scientific) for 30 min at room temperature. Spots were incubated for 30 min in blocking buffer (4% donkey serum (116-4101, Thermo Fisher Scientific) at room temperature. Primary antibodies (Table S1) in blocking buffer at the given concentration were incubated in a humidified chamber overnight at 4°C . Secondary antibodies (Table S2) supplemented with nuclear-staining DAPI (4',6-diamidino-2-phenylindole, Sigma-Aldrich) in blocking buffer were applied after washing steps (three times with PBS) and incubated for 60 min at room temperature. Spots were washed an additional 3 times in PBS.

Cell collection

To assemble completed DISCO devices, a top plate was joined by a spacer formed from two pieces of Scotch double-sided tape (3 M) with total spacer thickness of ~ 180 μm . $1\mu\text{L}$ of 0.005% 90R4 in distilled water was placed on each spot before assembly to ensure spot moisture. Lysis is achieved by firing one or more 8 ns pulses of the laser near the center of the selected cell at high power (4.5 μJ). After laser-lysis of 1-10 cells, 4 μL droplets of 0.005% 90R4 in distilled water were used to collect/wash the cell lysate and prepare the section for another round of laser-lysis.

DNA purification

DNA purification of bulk maternal and placenta samples were performed ~ 1 million cells according to the manufacturer's instructions. Low cell number (1-50 cells) samples were purified using Arcturus PicoPure kit (Applied Biosystems: 11815) according to the manufacturer's instructions. Qubit (Invitrogen: Q32854) was used to quantify DNA content according to the manufacturer's instructions.

Whole genome amplification and PCR

Whole genomic extracts from small pools of cells were generated using the PicoPure extraction kit (Thermo). DISCO collected samples containing 1-10 cells or dilute genomic DNA underwent whole genome amplification (WGA) using the Repli-g Single Cell Kit (Qiagen) following the manufacturer's instructions. Post reaction, the amplified product was heated at 65°C for 10 min and vortexed to resuspend and shear the long stranded genomic DNA and diluted 1:50 in ultrapure DI water. Chromosomal complement was initially assessed by PCR for loci on chromosomes X, 22, 4, 12, 13, and 22 (Sigma), using Taq DNA Polymerase (DreamTaq Green PCR

MasterMix 2X Invitrogen) according to the manufacturer's instructions. Products were evaluated by gel electrophoresis on a 4% w/v agarose gel, visualized using a Gel DocTM EZ Imaging System (Bio-Rad). Samples with at least 4 of the 5 expected loci were carried forward through the pipeline (with others discarded).

The presence of fetal DNA in male samples was assessed by PCR for the SRY loci. Control maternal vaginal epithelium and male control DNA were run with fetal samples. qPCR for Y chromosome DNA was performed using PowerQuant (Promega: PQ5008) and Applied Biosystems QuantStudio 6 (Thermo-Fisher) as per manufacturer's instructions and as described previously. PCR data was exported and analyzed using Promega PowerQuant Analysis Software.

Library preparation, SNP sequencing and nanopore sequencing

Placental and transcervical swab maternal sample DNA were extracted using the Arcturus PicoPure kit as previously described. Prospective fetal sample pools were composed of 3, 3, 5, and 5 isolated cells respectively and were subjected to whole genome amplification as previously described. Genomic DNA libraries were prepared from fetal cell samples using the V14 nanopore ligation sequencing kit (SQK-LSK114, Oxford Nanopore Technologies (ONT)). SNP libraries were prepared using rhAmpSeq Sample ID targeted amplicon sequencing panel (Integrated DNA Technologies). The Sample ID panel targets 71 human SNPs with high population polymorphism as well as 5 sex chromosome regions (2 X and 3 Y). Library concentrations were quantified by Qubit. Each Flongle flow cell (FLO-FLG114) was primed according to the manufacturer's guidelines before loading with a mix containing 5 μ l of diluted library (5 fmol) as per the manufacturer's instructions. Each library was sequenced on the Flongle flow cells for 48 hours. Alignment was performed with minimap2 to the target regions on the human genome reference hg38.⁴¹ Pysam was used to generate pileups on SNP regions, filtered to remove reads with base quality scores below 10 and mapping quality scores below 60.³⁹ Maternal and fetal genotypes are listed in Table S4. Fetal specific SNPs in collected samples were identified from placental controls with a minimum 1% variance as outside maternal sample SNP proportions.

Samples and library preparation for 10x RNA sequencing

4 transcervical swab samples were transferred to 50mL falcon tubes and centrifuged at 300xg for 10 minutes to collect any cells in the supernatant. PBS volume was adjusted to 25 mL and 25 mL of DMEM with dithiothreitol (DTT), sodium bicarbonate (Na₂CO₃) and Benzonase[®] was added to a final concentration of 10 mM DTT, 1 mM Na₂CO₃, and 28 mU Benzonase[®] to remove mucus. Samples were placed on a variable speed rocker (BR2000-GM 2D rocker, VWR) for 30 minutes at 37°C. Samples were centrifuged at 300xg for 10 minutes to collect transcervical swabs in solution.

Placental tissue was collected from pregnancy termination. Gestational age week 7.6 placental tissue was dissociated with trypsin for 30 minutes at 37°C. Cell suspension was filtered through a 40 μ m filter to remove clumps of tissue. Cellular suspension was centrifuged at 300xg for 10 minutes to collect placental cells in solution. 10X Chromium single-cell libraries were sequenced (Novaseq 6000, 100 cycles) at the Princess Margaret Genomics Center, University Health Network (Toronto, Canada). RNA sequencing data have been deposited at ArrayExpress and are publicly available as of the date of publication. Accession number: E-MTAB-15846, <https://www.ebi.ac.uk/biostudies/ArrayExpress/studies/E-MTAB-15846?key=d333677d-0aa8-44cb-8125-b8e11ac9271f>.

QUANTIFICATION AND STATISTICAL ANALYSIS

10x RNA sequencing analysis

The data were filtered to remove low-quality reads and then aligned to the human reference genome (hg38) using Cell Ranger. Cells were sorted according to the barcodes and the unique molecular identifiers (UMIs) were counted per gene for each cell. Cells passing QC were analyzed using Seurat^{42,43} v3.1.2. Counts were normalized and standardized using the NormalizeData and ScaleData function.

The input dataset for dimensionality reduction consists of the 20000 most variably expressed genes, as determined by the Seurat function FindVariableFeatures.³⁸ Transcervical swabs were jointly analysed using Seurat but separate from placental datasets. Datasets were visualised using PCA and UMAP on the corrected gene expression matrix. Unbiased clustering was performed using the FindClusters and Findneighbours functions. Lineage markers for annotation were identified using the FindMarkers function on the 10,000 integration genes. Marker expression of key markers was visualized using a scatter plot on UMAP or heatmaps.

Epithelial cell identities were extracted from transcervical swab datasets and subsequently renormalized and standardized using the NormalizeData and ScaleData function. Diffusion maps were generated using destiny v 2.12.0.⁴⁴

Fetal cell panel generation

To identify prospective fetal cells in transcervical swab datasets, transcervical swab cervical epithelial clusters and placental trophoblast clusters were combined into a single Seurat object. The merged dataset was renormalized and standardized using the NormalizeData and ScaleData function. Datasets were visualised using PCA and UMAP on the corrected gene expression matrix. Unbiased clustering was performed using the FindClusters and Findneighbours functions. Lineage markers for annotation were identified using the FindMarkers function on the 10,000 integration genes. Marker expression of key fetal markers was visualized using a scatter plot on UMAP or heatmaps.

Cluster 4 was identified as containing transcervical swab cells and trophoblast cells. The Findmarkers function was utilized to identify differentially expressed genes between cluster 4 and cervical epithelial clusters 3. Differentiating markers between trophoblast and cervical epithelium were similarly identified using Findmarkers comparing the trophoblast enriched cluster 1 to the cervical epithelium clusters. Final marker genes were selected by identifying genes overlapping between trophoblast enriched gene set and cluster 4 enriched genes. Significantly enriched genes were trimmed using an adjusted p value cut off <0.001 , an average fold change >2 , and expression in at least 25% of cells within a given cluster.

Scripts utilized in marker panel generation and analysis are available online: <https://github.com/DylanSiriwardena/DISCOdiagnostics>.

Image analysis

Background intensity was equalized between channels to normalize for non-specific secondary antibody binding to hydrophilic spots via gain/brightness adjustments for the entire experimental cohort. Images were analysed using the open-source software Fiji⁴⁵ to extract signal intensities and cell size. DAPI was used to generate a nuclei segmentation mask, while bright field and CK7 were utilized for cellular size measurements. CK7+ TFAP2A+ cells were identified from 1,224 imaged and segmented cells and CK7+ VGLL1+ cells were identified from 6,973 imaged and segmented cells. Statistical analysis of quantified fluorescent intensities were performed in R. Two-tailed Mann–Whitney test was used to compare between two means for samples that were not normally distributed.

qPCR analysis

Mean Y/Auto and Y/Deg were calculated from ratios of each respective CT value. Statistical analysis of quantified fluorescent intensities were performed in R and graphpad. Two-tailed t-test was used to compare between two means for samples. Further details can be found in figure captions.